



Characterization of Light-Enhanced Respiration in Cyanobacteria

Shimakawa, Ginga
Kohara, Ayaka
Miyake, Chikahiro

(Citation)

International Journal of Molecular Sciences, 22(1):342-342

(Issue Date)

2021-01

(Resource Type)

journal article

(Version)

Version of Record

(Rights)

© 2020 by the authors. Licensee MDPI, Basel, Switzerland.

This article is an open access article distributed under the terms and conditions of the Creative Commons Attribution (CC BY) license (<https://creativecommons.org/licenses/by/4.0/>).

(URL)

<https://hdl.handle.net/20.500.14094/90007809>





Article

Characterization of Light-Enhanced Respiration in Cyanobacteria

Ginga Shimakawa ^{1,*}, Ayaka Kohara ^{1,†} and Chikahiro Miyake ^{1,2}

¹ Department of Biological and Environmental Science, Faculty of Agriculture, Graduate School of Agricultural Science, Kobe University, 1-1 Rokkodai, Nada, Kobe 657-8501, Japan; a.kohara1199@gmail.com (A.K.); cmiyake@hawk.kobe-u.ac.jp (C.M.)

² Core Research for Environmental Science and Technology, Japan Science and Technology Agency, 7 Goban, Chiyoda, Tokyo 102-0076, Japan

* Correspondence: ginshimakawa@gmail.com; Fax: +81-78-803-5851

† These authors contributed equally to this paper.

‡ Current address: Research Center for Solar Energy Chemistry, Osaka University, 1-3 Machikaneyama, Toyonaka, Osaka 560-8631, Japan.

Abstract: In eukaryotic algae, respiratory O₂ uptake is enhanced after illumination, which is called light-enhanced respiration (LER). It is likely stimulated by an increase in respiratory substrates produced during photosynthetic CO₂ assimilation and function in keeping the metabolic and redox homeostasis in the light in eukaryotic cells, based on the interactions among the cytosol, chloroplasts, and mitochondria. Here, we first characterize LER in photosynthetic prokaryote cyanobacteria, in which respiration and photosynthesis share their metabolisms and electron transport chains in one cell. From the physiological analysis, the cyanobacterium *Synechocystis* sp. PCC 6803 performs LER, similar to eukaryotic algae, which shows a capacity comparable to the net photosynthetic O₂ evolution rate. Although the respiratory and photosynthetic electron transports share the interchain, LER was uncoupled from photosynthetic electron transport. Mutant analyses demonstrated that LER is motivated by the substrates directly provided by photosynthetic CO₂ assimilation, but not by glycogen. Further, the light-dependent activation of LER was observed even with exogenously added glucose, implying a regulatory mechanism for LER in addition to the substrate amounts. Finally, we discuss the physiological significance of the large capacity of LER in cyanobacteria and eukaryotic algae compared to those in plants that normally show less LER.

Keywords: oxygen; light-enhanced respiration; photosynthesis; respiratory terminal oxidases



Citation: Shimakawa, G.; Kohara, A.; Miyake, C. Characterization of Light-Enhanced Respiration in Cyanobacteria. *Int. J. Mol. Sci.* **2021**, *22*, 342. <https://doi.org/10.3390/ijms22010342>

Received: 6 November 2020

Accepted: 28 December 2020

Published: 31 December 2020

Publisher's Note: MDPI stays neutral with regard to jurisdictional claims in published maps and institutional affiliations.



Copyright: © 2020 by the authors. Licensee MDPI, Basel, Switzerland. This article is an open access article distributed under the terms and conditions of the Creative Commons Attribution (CC BY) license (<https://creativecommons.org/licenses/by/4.0/>).

1. Introduction

Respiration is one of the most important biological activities, even in oxygenic phototrophs that produce NAD(P)H and ATP by photosynthetic metabolism. In plants, algae, and cyanobacteria, respiratory metabolism and electron transport systems are mostly conserved, except for some components [1,2]. In principle, respiration plays a role in producing ATP outside of chloroplasts, in the nonphotosynthetic tissues and under nonphotosynthetic conditions (i.e., darkness). However, it has been broadly suggested that respiration also interacts with photosynthesis during illumination of redox, metabolic, and energetic events in photosynthetic organisms [3–9]. The phenotypes of various respiratory mutants indicate that the interplay between respiration and photosynthesis is essential for the growth of photosynthetic organisms [10–12].

Physiological functions of respiration in association with photosynthesis have not yet been fully understood in photosynthetic organisms. In a variety of eukaryotic algae, the O₂ uptake rate during dark respiration is frequently higher after illumination and can then reach about half of the photosynthetic O₂ evolution rate. The light-enhanced dark respiration (here we termed it as light-enhanced respiration, LER), one of the most indisputable phenomena that shows respiration is linked to photosynthesis under light conditions, is associated with the amounts of respiratory substrates generated during

photosynthesis in eukaryotic algae [4,13–16]. However, the details of the initiation and relaxation mechanism of LER are still unclear.

The interaction between respiration and photosynthesis has already been established in cyanobacteria, the prokaryotic algae broadly recognized as the progenitor of oxygenic photosynthesis [17–19]. Due to the lack of organelles, both respiration and photosynthesis proceed in one cell, and they both depend on the cytosolic metabolism and on the electron transport chain in the thylakoid membrane (Figure 1). The redox states of the photosynthetic electron transport components and the amounts of photosynthetic metabolites are affected in respiratory mutants [20–26], the interplay between respiration and photosynthesis in cyanobacterial cells. In the cyanobacterium *Synechocystis* sp. PCC 6803 (S. 6803), dark respiration starts from the degradation of glycogen catalyzed by debranching enzyme- or phosphorylase-dependent pathways [27,28]. Hexoses such as glucose are metabolized to pyruvate in the cytosol via glycolysis, similar to photosynthetic eukaryotes, and then drive the cyanobacterial tricarboxylic acid (TCA) cycle in the cytosol. Unique metabolic pathways in the cyanobacterial TCA cycle are still being uncovered, but the TCA cycle is likely to be the dominant source of NAD(P)H for the respiratory electron transport chain [29,30]. Meanwhile, in cyanobacteria oxidative the pentose phosphate pathway is also suggested to be an important source for reducing power, especially NADPH [31]. The thylakoid membrane contains both the photosynthetic and respiratory electron transport chains, both of which contribute to ATP production catalyzed by ATP synthase [32,33]. In the photosynthetic electron transport chain, the electrons generated by H₂O oxidation at photosystem II (PSII) are transported to NADP⁺ at the electron acceptor side of PSI. In the respiratory electron transport, the electrons are transported from NAD(P)H dehydrogenase (NDH)-1, NDH-2, and succinate dehydrogenase (SDH) to cytochrome *c* oxidase (COX), reducing O₂ to H₂O. These two electron transport chains share the interchain components plastoquinone (PQ), the cytochrome *b₆/f* complex, plastocyanin, and cytochrome *c* [18,22]. Additionally, in S. 6803, the cytochrome *bd*-type quinol oxidase complex (Cyd) reduces O₂ to H₂O using the electrons from plastoquinol [34]. Furthermore, akin to Cyd, the alternative respiratory terminal oxidase (ARTO) on the plasma membrane is reported to reduce O₂ [35]. In addition to ARTO, some respiratory electron transport components also function on the plasma membrane, separate from photosynthetic electron transport, details of which remain debatable [22,33]. Despite the prokaryotic characteristics, the physiological functions of respiration under light conditions are still unclear, and the notable phenomenon, LER, has never been targeted in cyanobacteria. Here, we first characterize LER in S. 6803 to deepen the understanding on the molecular mechanism of the interactions between respiration and photosynthesis in photosynthetic organisms.

2. Results

2.1. Relationship of Light-Enhanced Respiration with Photosynthesis in S. 6803

Since LER is activated by illumination, it is difficult to analyze the capacity of LER in photosynthetic organisms that are already adapted to light. To maximize the observed capacity of LER, in this study, cyanobacterial cells were adapted to darkness for 24 h in advance to physiological measurements (see Section 4). After the long dark adaptation, almost all of the respiratory substrates were assumed to be consumed, and the dark respiration rate was approximately 5 µmol O₂ mg chlorophyll (Chl)^{−1} h^{−1} (Figure 2), which was lower than the values previously reported for the wild type S. 6803 [21]. Upon illumination, net photosynthetic O₂ evolution was observed, but the rate gradually decreased from 80 to 50 µmol O₂ mg Chl^{−1} h^{−1} during illumination (Figure 2). After the actinic light was switched off, the O₂ uptake rate was approximately 40 µmol O₂ mg Chl^{−1} h^{−1}, which was designated as LER in this study. The LER was relieved within 20 min, and finally, the O₂ uptake rate was close to 10 µmol O₂ mg Chl^{−1} h^{−1} (Figure 2 and Figure S1), which was consistent with the values previously detected in the S. 6803 wild type [21].

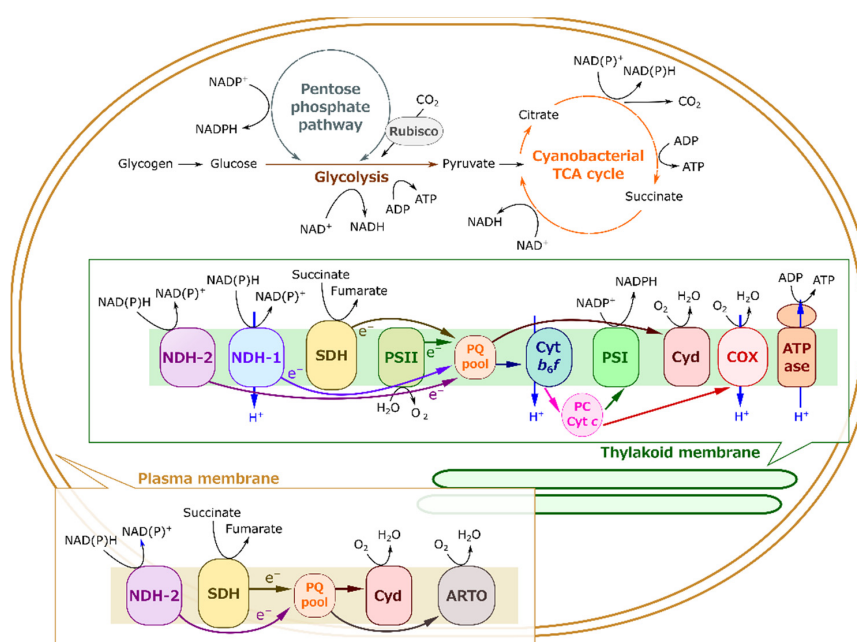


Figure 1. A brief illustration of respiration and photosynthesis sharing their metabolisms and electron transport chains in one cyanobacterial cell. To simplify the illustration, stoichiometry of each reaction and many bypasses are disregarded here. The direction of the arrows mainly follows the respiration mode. Under light conditions, photosynthetic electron transport proceeds from PSII to PSI, and Rubisco assimilates CO₂ to initiate the reductive pentose phosphate pathway (also called the Calvin–Benson cycle). Conversely, the oxidative pentose phosphate pathway proceeds in sugar catabolism, producing reducing power as NADPH. Abbreviations for enzymes and the complexes are as follows: Rubisco, ribulose 1,5-bisphosphate carboxylase/oxygenase; NDH-1 and -2, type I and II NAD(P)H dehydrogenase; SDH, succinate dehydrogenase; PSII and PSI, photosystem II and I; PQ, plastoquinone; Cyt *b₆f*, cytochrome *b₆f* complex; PC, plastocyanin; Cyt *c*, cytochrome *c*; Cyd, cytochrome *bd*-type quinol oxidase; COX, cytochrome *c* oxidase; ATPase, ATP synthase; ARTO, alternative respiratory terminal oxidase.

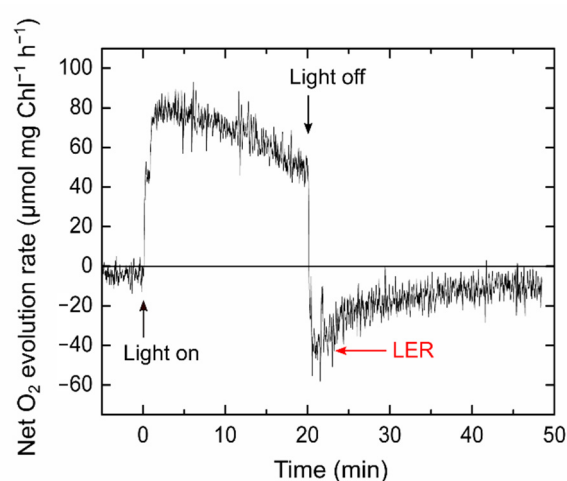


Figure 2. Light-enhanced respiration (LER) in *Synechocystis* sp. PCC 6803. The cyanobacterial cells adapted to darkness for 24 h (10 μg Chl mL⁻¹) were illuminated with a red actinic light (190 μmol photons m⁻² s⁻¹) for 20 min as indicated by black arrows. We defined the O₂ uptake rate just after the light was turned off as LER (red arrow). The representative data (*n* = 9, biological replicates) are shown.

Next, we analyzed LER after different illumination periods. Contrary to the decrease in net photosynthetic O₂ evolution rate, a increase in LER was observed with the time of illumination (Figure 3A). If any O₂-dependent alternative electron transports do not

compete with the CO_2 assimilation in this situation, the sum of net O_2 evolution and LER rates can be defined as the total photosynthetic O_2 evolution rate corresponding to the gross photosynthetic activity. The total photosynthetic O_2 evolution rate was kept almost constant and correlated with the effective quantum yield of PSII, $Y(\text{II})$, during illumination (Figure 3B). Overall, the decrease in the net O_2 evolution rate reflected the increase in LER but not an inactivation of CO_2 assimilation.

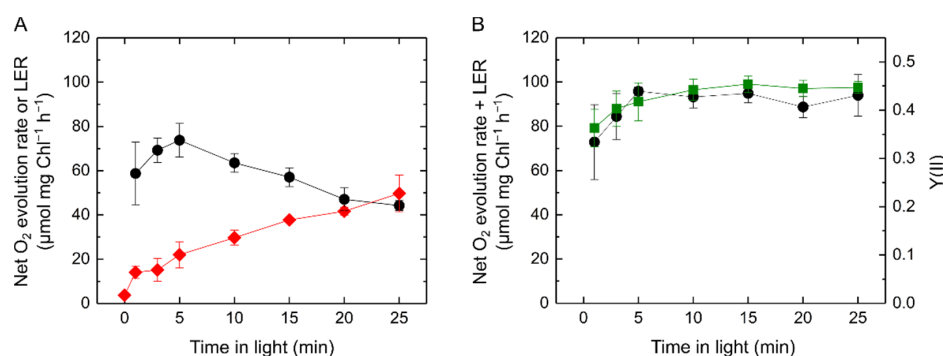


Figure 3. Light-enhanced respiration (LER) at different illumination times in *Synechocystis* sp. PCC 6803 adapted to the darkness for 24 h ($10 \mu\text{g Chl mL}^{-1}$). (A) Net O_2 evolution rate (black circles) and LER (red diamonds) by the illumination with a red actinic light ($190 \mu\text{mol photons m}^{-2} \text{s}^{-1}$). (B) Comparison of the total photosynthetic O_2 evolution rate (black circles) defined as the sum of net O_2 evolution rate and LER with effective quantum yield of photosystem II, $Y(\text{II})$ (green squares). Data are shown as the mean with the standard deviation ($n = 4$, biological replicates).

Further, the relationship of LER with the total photosynthetic O_2 evolution rate was evaluated after a 10 min illumination with the actinic light at various light intensities in *S. 6803* (Figure 4). The proportional relationship between LER and the total photosynthetic O_2 evolution rate indicates that LER is activated, paralleled with the photosynthetic CO_2 assimilation. In this study, LER was also observed in the other cyanobacterial strain *Synechococcus elongatus* PCC 7942 (S. 7942), also showing the proportional relationship between LER and the total photosynthetic O_2 evolution rate (Figure 4). As a result, LER is likely to be a common phenomenon in cyanobacteria. However, the capacity of LER, based on the photosynthetic activity, was larger in *S. 7942* than in *S. 6803* (Figure 4).

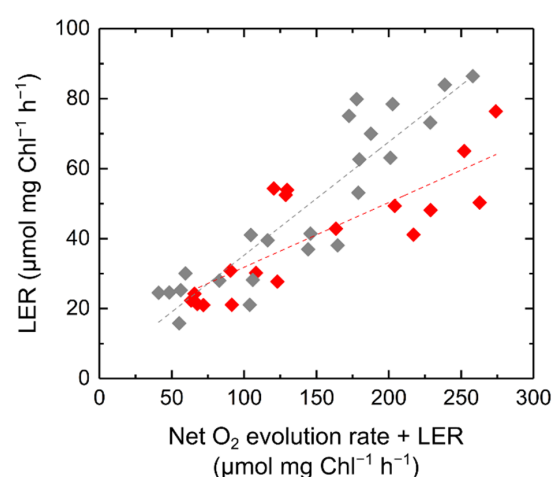


Figure 4. Relationship of light-enhanced respiration (LER) with the total photosynthetic O_2 evolution rate defined as the sum of net O_2 evolution rate and LER in *Synechocystis* sp. PCC 6803 (red) and *Synechococcus elongatus* PCC 7942 (grey) adapted to the darkness for 24 h. The cyanobacterial cells ($10 \mu\text{g Chl mL}^{-1}$) were illuminated with a red actinic light for 10 min at 90 ($n = 4$), 190 ($n = 7$), 400 ($n = 3$), and 600 ($n = 4$) $\mu\text{mol photons m}^{-2} \text{s}^{-1}$ (biological replicates). Dashed lines represent the estimated linear regressions of the data (*S. 6803*, $R^2 = 0.6586$; *S. 7942*, $R^2 = 0.8305$).

2.2. Molecular Mechanism of Light-Enhanced Respiration in *S. 6803*

The correlation between LER and illumination time suggests that LER was motivated by reducing cofactors or metabolites generated during photosynthesis in the cyanobacterium *S. 6803*. We constructed the *S. 6803* mutants deficient in respiratory components encoded in *cox* (COX), *cyd* (Cyd), *arto* (ARTO), *glgP* (glycogen phosphorylases), and *glgX* (glycogen debranching enzymes) to investigate the molecular mechanism of LER in *S. 6803* (Figure S2). In Figure 5A, we show the LER activity upon switching the actinic light off after 20 min of illumination in the wild type of *S. 6803*, the triple mutant for respiratory terminal oxidases ($\Delta cox/cyd/arto$), and the quadruple mutant for glycogen phosphorylases and blanching enzymes ($\Delta glgP1/glgP2/glgX1/glgX2$, termed $\Delta glgP/glgX$). These respiratory mutants show a trend of lower dark respiration than the wild type before the illumination (Figure 5A). The capacity of LER was significantly lower in $\Delta cox/cyd/arto$, but not different in $\Delta glgP/glgX$ compared to the wild type (Figure 5). In $\Delta cox/cyd/arto$, approximately 60% of the capacity was lost, but a part of the LER was still detected even in this mutant (Figure 5A). Nevertheless, there was only a minimal change in the net O_2 evolution rate in $\Delta cox/cyd/arto$ after the actinic light was turned off, suggesting that the transient increase in O_2 uptake was almost derived from these respiratory terminal oxidases (Figure 5B and Figure S1). It has been suggested that a leak of electrons to O_2 in the dark produces reactive oxygen species in a light–dark cycle in the *S. 6803* mutants deficient in respiratory terminal oxidases [22], which may partially contribute to the O_2 uptake observed in $\Delta cox/cyd/arto$ (Figure 5A).

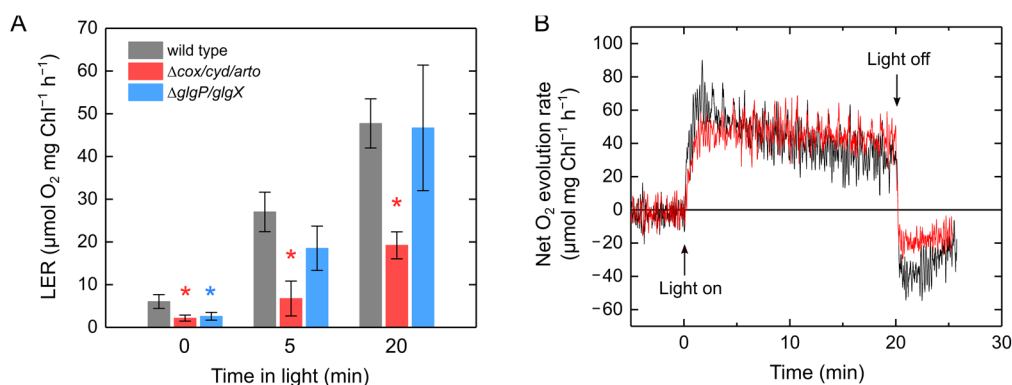


Figure 5. Light-enhanced respiration (LER) in wild type (grey bars) and the mutant of *Synechocystis* sp. PCC 6803 deficient in respiratory terminal oxidases ($\Delta cox/cyd/arto$, red bars) and glycogen degradation enzymes ($\Delta glgP/glgX$, blue bars) adapted to the darkness for 24 h. (A) LER after 20 min illumination with a red actinic light ($190 \mu\text{mol photons m}^{-2} \text{s}^{-1}$). Data are shown as the mean with the standard deviation ($n = 4$, biological replicates). Asterisks indicate statistically significant differences ($p < 0.05$) between wild type and the mutants as per Student's *t*-test. (B) Representative comparison of the net O_2 evolution rate in the wild type (black) with that in the $\Delta cox/cyd/arto$ (red).

We also analyzed LER in the *S. 6803* mutants deficient in components related to O_2 -dependent alternative electron transport [36,37]. Flavodiiron proteins (FLVs) function as alternative electron sinks at the electron acceptor side of PSI to dissipate the excess electrons from reducing ferredoxin to O_2 in *S. 6803* [38,39]. Disruption of FLV had no effect on LER (Figure 6A). Further, we also assessed the possibility that photorespiration partially contributes to LER. In all plants, except the C_4 plants, postillumination transient O_2 uptake is largely observed at a CO_2 compensation point and is driven by photorespiration [40,41]. In *S. 6803*, similar to eukaryotic algae [14], the capacity of LER was rather low under CO_2 limitation, and there was no difference between the wild type and the photorespiratory mutant deficient in glycolate dehydrogenase (Figure 6B). Overall, these mutant analyses suggested that O_2 -dependent alternative electron transport such as FLV-mediated Mehler-like reactions and photorespiration are not included in the LER.

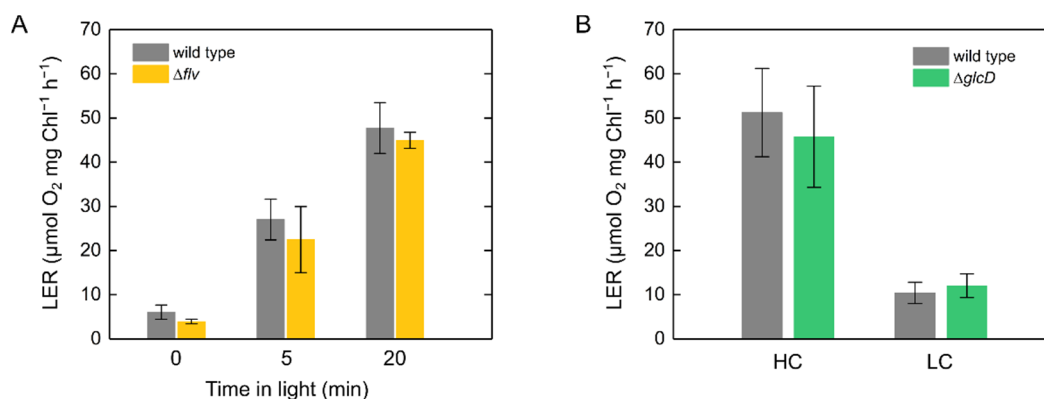


Figure 6. Light-enhanced respiration (LER) in wild type (grey bars) and the mutants of *Synechocystis* sp. PCC 6803 deficient in components related to alternative electron transport pathways. **(A)** LER in the mutant that lacks flavodiiron proteins 1, 3, and 4 (Δflv , yellow bars). **(B)** LER in the mutant deficient in glycolate dehydrogenase 1 and 2 ($\Delta gldD$, green bars). In “HC (high CO₂)”, cyanobacterial cells adapted to the darkness for 24 h ($10 \mu\text{g Chl mL}^{-1}$) were illuminated with red actinic light ($190 \mu\text{mol photons m}^{-2} \text{ s}^{-1}$) for 20 min, as in the LER measurements in the other strains. The “LC (low CO₂)” indicates the condition where available CO₂ is limited, which was prepared by a long-term (1–2 h) illumination without adding NaHCO₃ to the oxygen electrode chamber (Shimakawa et al., 2015). The actinic light was turned off at the steady state under CO₂ limitation, and then LER was measured. Data are shown as the mean with the standard deviation ($n = 4$, biological replicates).

To investigate the effects of the respiratory substrates on LER in *S. 6803*, we exogenously added glucose (final concentration, 5 mM) 10 min before illumination. The cyanobacterium *S. 6803* can take up exogenous glucose as a respiratory substrate to accumulate a variety of intermediates in the glycolysis and the Calvin–Benson cycle [21]. In fact, the dark respiration rate increased to approximately $20 \mu\text{mol O}_2 \text{ mg Chl}^{-1} \text{ h}^{-1}$ in the presence of glucose (Figure 7). We confirmed that the dark respiration rate did not further increase with 15 mM glucose, indicating that 5 mM glucose causes enough saturation to enhance the dark respiration in *S. 6803*. The amount of glucose consumed by LER is roughly estimated from the O₂ consumption—for example, in Figure 2, it can be seen that only $8 \mu\text{M}$ was produced by 10 min in dark. We note that the exogenous addition of glucose does not necessarily mimic the situation where the whole pool of respiratory substrates is saturated. Although the capacity of LER was greater with exogenously added glucose, light-dependent activation was observed, as was the case without glucose (Figures 3A and 7B). Overall, the increase in LER paralleled with photosynthesis can not only be explained by the amounts of respiratory substrates. The effect of exogenous glucose on LER was also investigated at various light intensities of the actinic light. Even in the presence of glucose, the capacity of LER increased with the light intensity as in the manner without glucose (Figure S3), which also suggested that there is a certain impact of light on increasing the LER capacity regardless of the amount of glucose.

We further tested the relaxation of the effect of exogenous glucose on LER in the darkness. Although net O₂ uptake rate reached approximately $50 \mu\text{mol O}_2 \text{ mg Chl}^{-1} \text{ h}^{-1}$ after the 10 min illumination with actinic light in the presence of glucose (Figure 7B), it decreased to $20 \mu\text{mol O}_2 \text{ mg Chl}^{-1} \text{ h}^{-1}$ if glucose was added 70 min after the actinic light was turned off (Figure 8A), which was almost the same value as that from when glucose was added before the illumination (Figure 7). Here, we hypothesize an elusive light-dependent activation step of LER and assessed the relaxation by adding glucose at different times in dark after the 10 min illumination (Figure 8B), indicating that the stimulation of O₂ uptake by exogenous glucose was enhanced by the illumination and slowly relaxed in dark to a constant level in approximately 1 h.

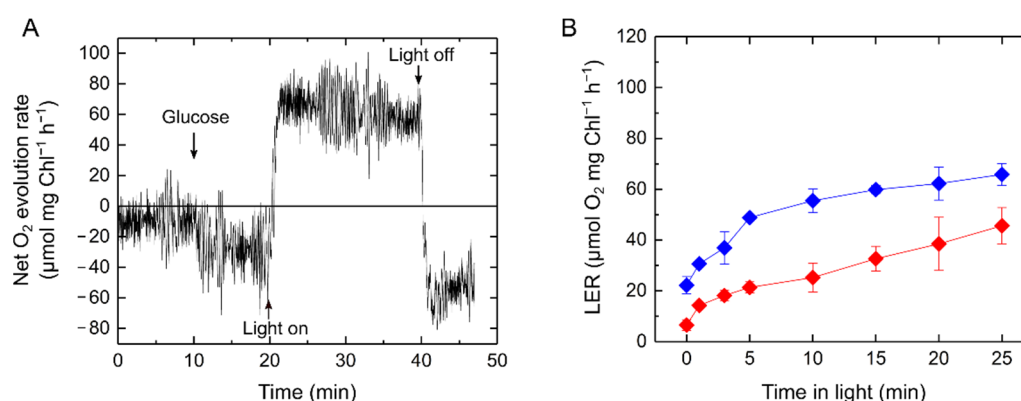


Figure 7. Effects of exogenously added glucose on light-enhanced respiration (LER) in *Synechocystis* sp. PCC 6803 adapted to the darkness for 24 h (A). Representative data of net O₂ evolution rate in response to the illumination with a red actinic light (190 μmol photons m⁻² s⁻¹). Glucose (5 mM) was exogenously added 10 min before the start of the illumination as indicated by a black arrow (B). LER at different illumination times in the absence (red) and presence (blue) of glucose. Data are shown as the mean with the standard deviation ($n = 3$, biological replicates).

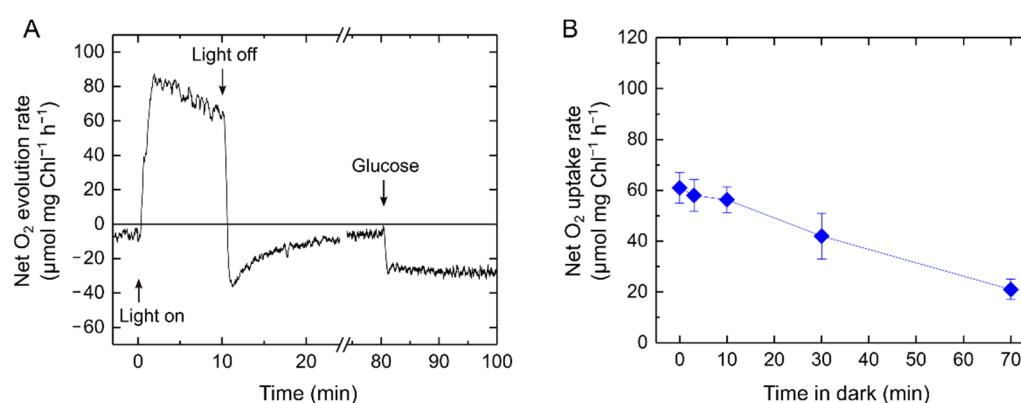


Figure 8. Relaxation of effects of exogenously added glucose on light-enhanced respiration (LER) in the darkness in *Synechocystis* sp. PCC 6803. The cyanobacterial cells adapted to darkness for 24 h (10 μg Chl mL⁻¹) were illuminated with a red actinic light (190 μmol photons m⁻² s⁻¹) for 10 min. (A) Representative data of net O₂ evolution rate in response to the illumination with the actinic light and the addition of glucose (5 mM) as indicated by arrows. (B) Net O₂ uptake rate stimulated by the addition of glucose at different times after the actinic light was turned off. At time zero, glucose was exogenously added and then the O₂ uptake was measured just after the 10 min illumination with the actinic light. Data are shown as the mean with the standard deviation ($n = 3$, biological replicates).

3. Discussion

3.1. Cyanobacterial Light-Enhanced Respiration Is Metabolically Coupled with Photosynthesis

Simultaneously with the evolution of PSII, O₂ is consumed under light through respiration, photorespiration, and an FLV-mediated Mehler-like reaction [42]. The large amount of O₂ consumed after an actinic light is turned off corresponds to the amount of substrate for respiration or photorespiration produced in the light [41]. Therefore, the analysis of postillumination transient O₂ uptake is a useful method to uncover the molecular mechanism of O₂-consuming reactions during photosynthesis. Whereas in plant leaves the postillumination transient O₂ uptake is dominantly driven by photorespiration under CO₂ limitation [40,41], in eukaryotic algae it is mainly derived from LER where enough CO₂ is available [14,16]. Here, we analyzed the postillumination transient O₂ uptake in cyanobacteria and found that it is derived from LER, similar to eukaryotic algae, and is associated with photosynthesis (Figures 3 and 4). In cyanobacteria, respiration and photosynthesis both depend on their metabolism, electron transport, and redox signaling in

one cell. Due to the sharing of the interchain components, the redox states of PQ, PSI, and NADP⁺ are potentially affected by defects in the respiratory electron transport components in the darkness and light–dark transition [20,43,44]. In this study, we observed O₂ uptake rate of LER that can be comparable to the net photosynthetic O₂ evolution rate (Figure 2). The increase in LER caused the decrease in net O₂ evolution rate (Figure 3A). The sum of net O₂ evolution and LER was coupled with Y(II) (Figure 3B). Overall, the large capacity of LER originated from the respiratory electron transport chain driven by substrates produced in the Calvin–Benson cycle, but not by an electron leakage from photosynthetic electron transport chain on the thylakoid membrane. This conclusion was consistent with the results of mutant analyses (Figures 5 and 6) and is in agreement with the fact that the electron sink capacity of the alternative electron transport from PSII to respiratory terminal oxidases is not significant in light, compared with photosynthetic linear electron flow and FLV-mediated electron transports [36,45]. Based on the present dataset, we cannot exclude the possibility that the LER measured after the actinic light was turned off did not necessarily reflect the exact respiratory O₂ uptake during illumination since the membrane potential, also called *proton motive force*, depends on both the respiratory and photosynthetic electron transport chains in the thylakoid membrane [46], which possibly suppresses the respiratory electron transport via “back-pressure” of the *proton motive force* [47]. Meanwhile, the net O₂ evolution rate decreased with Y(II) being kept constant (Figures 2 and 3), supporting the hypothesis that LER exactly occurs during the illumination.

3.2. Cyanobacterial Light-Enhanced Respiration Is Not Restricted Only to Respiratory Substrate Amounts

Characterization of LER in S. 6803 led us to analyze the respiratory mutants $\Delta\text{cox}/\text{cyd}/\text{arto}$ and $\Delta\text{glgP}/\text{glgX}$. The same extent of LER in $\Delta\text{glgP}/\text{glgX}$ as in the wild type clearly indicated that LER requires substrates derived not from glycogen, but directly from the Calvin–Benson cycle. There are several possibilities for electron donation from the stroma to the respiratory electron transport chain. The amounts of specific substrates can be an important factor for enhancing and suppressing respiration. For example, it has recently been reported that the NADPH-generating enzymes in the oxidative pentose phosphate pathway are inhibited by the TCA cycle intermediate citrate in S. 6803, implying a regulation for balancing NAD(P)H production in cyanobacterial respiratory metabolism [48]. It may be reasonable to assume that the activities of some respiratory enzymes are strictly regulated by specific metabolites to control the complex mixture of various respiratory and photosynthetic metabolisms in one cyanobacterial cell. The addition of exogenous glucose increased the dark respiration rate, but it did not affect the light-dependent activation process of LER (Figure 7B and Figure S3), implying that the regulatory mechanism of cyanobacterial LER does not only depend on the amounts of respiratory substrates. Based on the experiments with exogenous glucose, the elusive light-dependent activation step almost finished within 20 min in light and was then slowly relaxed to a constant level within 1 h in dark. The redox state of the components related to photosynthetic electron transport (e.g., PQ) may function in regulating the capacity of LER through a signaling system. Meanwhile, we also note the possibility that LER is stimulated by a specific metabolite produced by photosynthesis in light, independently of the metabolism driven by glucose, in the same activation manner with and without exogenous glucose (Figure 7B and Figure S3).

3.3. Light-Enhanced Respiration Plays a Role in Producing ATP through Consumption of Photosynthates

It is assumed that the physiological significance of LER is the immediate production of ATP using excess photosynthates. In other words, ATP is additionally demanded even during photosynthesis, probably for a variety of cell metabolisms. The present study showed that the LER capacity in S. 6803 can reach approximately half of the total photosynthetic O₂ evolution rate, which is likely to be sufficient to consume excess organic acids produced by photosynthesis under light conditions. However, the cyanobacterium S. 7942 mutant deficient in glycogen synthesis excretes organic acids such as pyruvate and

2-oxoglutarate in the medium, thereby increasing the concentration of exogenous pyruvate at approximately 0.1 mM per day under nitrogen deprivation [49]. This implies that even at a greater capacity of LER, cyanobacteria assimilate CO₂ to sugars at a rate that is more than what is needed and store them in the form of glycogen during photosynthesis. Possibly, the higher photosynthetic productivity as opposed to the demand for cell growth could have led to the evolution of cyanobacteria to multicellular photosynthetic organisms.

3.4. Evolutionary Changes of Light-Enhanced Respiration and Photorespiration Capacities from Algae to Plants

In the present study, cyanobacteria possess a large capacity of LER, similar to eukaryotic algae, including green algae and a variety of secondary algae. That is, LER is a common phenomenon in prokaryotic and eukaryotic algae, even though there are variations in the capacities among species. Meanwhile, the capacity of LER is much lower in *in vivo* plant leaves. The difference between these unicellular algae and plant leaves could be due to the different sink capacities for photosynthates. In cyanobacteria and eukaryotic algae, the utilization of photosynthates can often be limited to carbon metabolism in cells, especially under higher light and CO₂ conditions. The productivity of photosynthetic CO₂ assimilation has been developed during the evolution of photosynthetic organisms to shallow and terrestrial fields, resulting in a higher accumulation of photosynthates. In particular, out of water, photosynthetic organisms can have difficulties in excreting excess photosynthates. These factors could explain why photosynthetic organisms evolved to multicellular formations and developed intercellular mass transfers to expand the carbon sink capacity. Contrary to the evolution of terrestrial plants in the photosynthetic green lineage, some cyanobacteria, such as *Prochlorococcus*, are likely to have adopted the strategy to develop carbon excretion for the acclimation to oceanic surface ecosystems [50].

In contrast to LER, photorespiration has increased the energetic and metabolic capacity reflected in the O₂ uptake in the evolutionary history from algae to plants [40]. In land plants, except for C₄ plants, the large capacity of postillumination transient O₂ uptake is observed under CO₂ limitation, which is different from cyanobacteria (Figure 6B) and eukaryotic algae [14]. Indeed, the O₂ uptake in plants mainly originates from photorespiration [41]. Although photorespiratory metabolism is almost conserved and plays an important role in the growth under CO₂ limitation in *S. 6803* [51], the electron flux capacity through photorespiration is negligible, as compared to the photosynthetic CO₂ assimilation [36], which was also demonstrated by the measurement of LER in the present study (Figure 6B).

4. Materials and Methods

4.1. Growth Conditions and Chl *a* Determination

The cyanobacterium *S. 6803* was cultured as described in our previous work [52]. Cells from the culture, with initial OD₇₅₀ of 0.1 to 0.2, were inoculated into liquid BG-11 medium and grown on a rotary shaker (100 rpm) under continuous fluorescent lighting (25 °C, 150 μmol photons m⁻² s⁻¹) at 2% (*v/v*) [CO₂]. The optical density of the medium was measured using a spectrophotometer (U-2800A, Hitachi, Tokyo, Japan). For all the physiological measurements of LER, cells from the exponential growth phase were adapted to the dark for 24 h before they were used.

For Chl measurement, cells from the 0.1 to 1.0 mL cultures were centrifugally harvested and resuspended by vortexing in 1 mL 100% (*v/v*) methanol. After incubation for 5 min in the dark, the suspension was centrifuged at 10,000 × *g* for 5 min. The total Chl *a* was spectrophotometrically determined from the supernatant [53].

4.2. Generation of Mutants

The mutants of *S. 6803*, Δ*cox/cyd*, Δ*glgP*, Δ*flv*, and Δ*glcD* were constructed in our previous studies [21,36,37,43]. To disrupt the genes *ctaCII* (*arto*; *slr0813*), *glgX1* (*slr0237*), and *glgX2* (*slr1857*) in *S. 6803*, each portion of the coding region was replaced with streptomycin and erythromycin resistance cassettes (*Sm^r* and *Em^r*), derived from pRL453 and pRL425,

respectively [54]. The triple mutant for the respiratory terminal oxidases was generated by the transformation of $\Delta\text{cox}/\text{cyd}$ with the *arto*-deleted construct containing Em^r . The quadruple mutant $\Delta\text{glgP}/\text{glgX}$ was generated by the two transformations of ΔglgP with the *glgX1*- and *glgX2*-deleted constructs containing Sm^r and Em^r . For the preparation of the construct with Sm^r , the coding region was cloned into a pTA2 vector (Toyobo, Otsu, Japan). The plasmid was linearized by inverse polymerase chain reaction (PCR) and ligated with Sm^r [55]. To prepare the constructs with Em^r , two separated PCR fragments for the coding regions were linked with Em^r by successive PCR [36,56]. Transformants were selected on 0.5% (*w/v*) agar plates of BG-11 medium containing antibiotics. Complete segregation of each mutant was confirmed by PCR (Figure S2). The primers used for the amplification of each region are shown in Table S1.

4.3. Measurement of O_2 and Chl Fluorescence

Net uptake and evolution of O_2 were measured concurrently with Chl fluorescence using a Clark-type O_2 electrode (Hansatech Instruments Ltd., King's Lynn, UK). Cell samples in the reaction mixture (2 mL, 50 mM HEPES-KOH, pH 7.5, 10 mM NaHCO_3 , 10 μg Chl mL^{-1}) were stirred with a magnetic microstirrer and illuminated with red actinic light ($\lambda > 620$ nm) at 25 °C. The photon flux densities are indicated in the figure legends. A halogen lamp (Xenophot HLX 64625, Osram, München, Germany) from an LS2 light source (Hansatech) was used as the red actinic light source. The rates of O_2 uptake and evolution were calculated from the change in the O_2 concentration in the mixture in 10 s (examples of raw traces are shown in Figure S1). The data points were acquired every second.

The relative Chl fluorescence originating from Chl *a* was measured using a PAM-Chl fluorometer (PAM-101; Walz, Effeltrich, Germany) as previously described [57]. Pulse-modulated excitation was achieved using an LED lamp with a peak emission at 650 nm. Modulated fluorescence was measured at $\lambda > 710$ nm (Schott RG9 long-pass filter; Walz). The steady-state fluorescence (F_s) was monitored under actinic light. To determine the maximum variable fluorescence in the light (F_m'), 1000 ms pulses of saturated light (10,000 μmol photons m^{-2} s^{-1}) were supplied. The fluorescence terminology used in this study follows the previous report [58]. $Y(\text{II})$, the effective quantum yield of PSII, was defined as $(F_m' - F_s)/F_m'$.

Supplementary Materials: The following are available online at <https://www.mdpi.com/1422-0067/22/1/342/s1>, Table S1: Primers used in this study; Figure S1: Examples of raw traces of the change in O_2 concentration in *Synechocystis* sp. PCC 6803 wild type and the mutant deficient respiratory terminal oxidases; Figure S2: Insertional inactivation of the genes for alternative respiratory terminal oxidase and glycogen deblanching enzymes in *Synechocystis* sp. PCC 6803; Figure S3: Net O_2 evolution rate and light-enhanced respiration in the 10 min illumination with actinic light at different light intensities in *Synechocystis* sp. PCC 6803 adapted to the darkness for 24 h.

Author Contributions: C.M. conceived the original screening and research plans; A.K. performed all the physiological measurements; G.S. provided A.K. with technical assistance and mutant strains; G.S., A.K., and C.M. designed the experiments and analyzed the data; G.S. wrote the manuscript. All authors have read and agreed to the published version of the manuscript.

Funding: This work was supported by Core Research for Evolutional Science and Technology of Japan Science and Technology Agency, Japan (grant number JPMJCR1503 to C.M.) and by Japan Society for the Promotion of Science (grant number 16J03443 and A20J001050 to G.S.).

Institutional Review Board Statement: Not applicable.

Informed Consent Statement: Not applicable.

Data Availability Statement: Not applicable.

Conflicts of Interest: The authors have no conflict of interest to declare.

References

1. Raven, J.A.; Beardall, J. Dark respiration and organic carbon loss. In *The Physiology of Microalgae*; Borowitzka, M.A., Beardall, J., Raven, J.A., Eds.; Springer International Publishing: Cham, Switzerland, 2016; pp. 129–140. [\[CrossRef\]](#)
2. Møller, I.M. Plant mitochondria and oxidative stress: Electron transport, NADPH turnover, and metabolism of reactive oxygen species. *Annu. Rev. Plant Physiol. Plant Mol. Biol.* **2001**, *52*, 561–591. [\[CrossRef\]](#) [\[PubMed\]](#)
3. Bailleul, B.; Berne, N.; Murik, O.; Petroustos, D.; Prihoda, J.; Tanaka, A.; Villanova, V.; Bligny, R.; Flori, S.; Falconet, D.; et al. Energetic coupling between plastids and mitochondria drives CO₂ assimilation in diatoms. *Nature* **2015**, *524*, 366–369. [\[CrossRef\]](#) [\[PubMed\]](#)
4. Raghavendra, A.S.; Padmasree, K. Beneficial interactions of mitochondrial metabolism with photosynthetic carbon assimilation. *Trends Plant Sci.* **2003**, *8*, 546–553. [\[CrossRef\]](#) [\[PubMed\]](#)
5. Sabar, M.; De Paepe, R.; de Kouchkovsky, Y. Complex I impairment, respiratory compensations, and photosynthetic decrease in nuclear and mitochondrial male sterile mutants of *Nicotiana sylvestris*. *Plant Physiol.* **2000**, *124*, 1239–1250. [\[CrossRef\]](#) [\[PubMed\]](#)
6. Massoz, S.; Larosa, V.; Horrion, B.; Matagne, R.F.; Remacle, C.; Cardol, P. Isolation of *Chlamydomonas reinhardtii* mutants with altered mitochondrial respiration by chlorophyll fluorescence measurement. *J. Biotechnol.* **2015**, *215*, 27–34. [\[CrossRef\]](#)
7. Lapaille, M.; Thiry, M.; Perez, E.; González-Halphen, D.; Remacle, C.; Cardol, P. Loss of mitochondrial ATP synthase subunit beta (Atp2) alters mitochondrial and chloroplastic function and morphology in *Chlamydomonas*. *Biochim. Biophys. Acta Bioenerg.* **2010**, *1797*, 1533–1539. [\[CrossRef\]](#)
8. Noguchi, K.; Yoshida, K. Interaction between photosynthesis and respiration in illuminated leaves. *Mitochondrion* **2008**, *8*, 87–99. [\[CrossRef\]](#)
9. Larosa, V.; Meneghesso, A.; La Rocca, N.; Steinbeck, J.; Hippler, M.; Szabò, I.; Morosinotto, T. Mitochondria affect photosynthetic electron transport and photosensitivity in a green alga. *Plant Physiol.* **2018**, *176*, 2305–2314. [\[CrossRef\]](#)
10. Tomaz, T.; Bagard, M.; Pracharoenwattana, I.; Lindén, P.; Lee, C.P.; Carroll, A.J.; Ströher, E.; Smith, S.M.; Gardeström, P.; Millar, A.H. Mitochondrial Malate Dehydrogenase Lowers Leaf Respiration and Alters Photorespiration and Plant Growth in *Arabidopsis*. *Plant Physiol.* **2010**, *154*, 1143–1157. [\[CrossRef\]](#)
11. Meyer, E.H.; Tomaz, T.; Carroll, A.J.; Estavillo, G.; Delannoy, E.; Tanz, S.K.; Small, I.D.; Pogson, B.J.; Millar, A.H. Remodeled respiration in *ndufs4* with low phosphorylation efficiency suppresses *Arabidopsis* germination and growth and alters control of metabolism at night. *Plant Physiol.* **2009**, *151*, 603–619. [\[CrossRef\]](#)
12. Stitt, M.; Zeeman, S.C. Starch turnover: Pathways, regulation and role in growth. *Curr. Opin. Plant Biol.* **2012**, *15*, 282–292. [\[CrossRef\]](#) [\[PubMed\]](#)
13. Mantikci, M.; Hansen, J.L.S.; Markager, S. Photosynthesis enhanced dark respiration in three marine phytoplankton species. *J. Exp. Mar. Biol. Ecol.* **2017**, *497*, 188–196. [\[CrossRef\]](#)
14. Weger, H.G.; Herzig, R.; Falkowski, P.G.; Turpin, D.H. Respiratory losses in the light in a marine diatom: Measurements by short-term mass spectrometry. *Limnol. Oceanogr.* **1989**, *34*, 1153–1161. [\[CrossRef\]](#)
15. Ekelund, N.G.A. Interactions between photosynthesis and ‘light-enhanced dark respiration’ (LEDR) in the flagellate *Euglena gracilis* after irradiation with ultraviolet radiation. *J. Photochem. Photobiol. B Biol.* **2000**, *55*, 63–69. [\[CrossRef\]](#)
16. Xue, X.; Gauthier, D.A.; Turpin, D.H.; Weger, H.G. Interactions between photosynthesis and respiration in the green alga *Chlamydomonas reinhardtii* (Characterization of light-enhanced dark respiration). *Plant Physiol.* **1996**, *112*, 1005–1014. [\[CrossRef\]](#)
17. Scherer, S.; Almon, H.; Böger, P. Interaction of photosynthesis, respiration and nitrogen fixation in cyanobacteria. *Photosynth. Res.* **1988**, *15*, 95–114. [\[CrossRef\]](#)
18. Peschek, G.A.; Obinger, C.; Paumann, M. The respiratory chain of blue-green algae (cyanobacteria). *Physiol. Plant.* **2004**, *120*, 358–369. [\[CrossRef\]](#)
19. Binder, A. Respiration and photosynthesis in energy-transducing membranes of cyanobacteria. *J. Bioenerg. Biomembr.* **1982**, *14*, 271–286. [\[CrossRef\]](#)
20. Mi, H.; Klughammer, C.; Schreiber, U. Light-induced dynamic changes of NADPH fluorescence in *Synechocystis* PCC 6803 and its *ndhB*-defective mutant M55. *Plant Cell Physiol.* **2000**, *41*, 1129–1135. [\[CrossRef\]](#)
21. Shimakawa, G.; Hasunuma, T.; Kondo, A.; Matsuda, M.; Makino, A.; Miyake, C. Respiration accumulates Calvin cycle intermediates for the rapid start of photosynthesis in *Synechocystis* sp. PCC 6803. *Biosci. Biotechnol. Biochem.* **2014**, *78*, 1997–2007. [\[CrossRef\]](#)
22. Lea-Smith, D.J.; Ross, N.; Zori, M.; Bendall, D.S.; Dennis, J.S.; Scott, S.A.; Smith, A.G.; Howe, C.J. Thylakoid terminal oxidases are essential for the cyanobacterium *Synechocystis* sp. PCC 6803 to survive rapidly changing light intensities. *Plant Physiol.* **2013**, *162*, 484–495. [\[CrossRef\]](#)
23. Ogawa, T.; Sonoike, K. Dissection of respiration and photosynthesis in the cyanobacterium *Synechocystis* sp. PCC6803 by the analysis of chlorophyll fluorescence. *J. Photochem. Photobiol. B Biol.* **2015**, *144*, 61–67. [\[CrossRef\]](#)
24. Feilke, K.; Ajlani, G.; Krieger-Liszka, A. Overexpression of plastid terminal oxidase in *Synechocystis* sp. PCC 6803 alters cellular redox state. *Philos. Trans. R. Soc. B Biol. Sci.* **2017**, *372*, 20160379. [\[CrossRef\]](#)
25. Ermakova, M.; Huokko, T.; Richaud, P.; Bersanini, L.; Howe, C.J.; Lea-Smith, D.J.; Peltier, G.; Allahverdiyeva, Y. Distinguishing the roles of thylakoid respiratory terminal oxidases in the cyanobacterium *Synechocystis* sp. PCC 6803. *Plant Physiol.* **2016**, *171*, 1307–1319. [\[CrossRef\]](#)
26. Mills, L.A.; McCormick, A.J.; Lea-Smith, D.J. Current knowledge and recent advances in understanding metabolism of the model cyanobacterium *Synechocystis* sp. PCC 6803. *Biosci. Rep.* **2020**, *40*, BSR20193325. [\[CrossRef\]](#)

27. Ball, S.G.; Morell, M.K. From bacterial glycogen to starch: Understanding the biogenesis of the plant starch granule. *Annu. Rev. Plant Biol.* **2003**, *54*, 207–233. [\[CrossRef\]](#)
28. Osanai, T.; Azuma, M.; Tanaka, K. Sugar catabolism regulated by light-and nitrogen-status in the cyanobacterium *Synechocystis* sp. PCC 6803. *Photochem. Photobiol. Sci.* **2007**, *6*, 508–514. [\[CrossRef\]](#)
29. Steinhauser, D.; Fernie, A.R.; Araújo, W.L. Unusual cyanobacterial TCA cycles: Not broken just different. *Trends Plant Sci.* **2012**, *17*, 503–509. [\[CrossRef\]](#)
30. Broddrick, J.T.; Rubin, B.E.; Welkie, D.G.; Du, N.; Mih, N.; Diamond, S.; Lee, J.J.; Golden, S.S.; Palsson, B.O. Unique attributes of cyanobacterial metabolism revealed by improved genome-scale metabolic modeling and essential gene analysis. *Proc. Natl. Acad. Sci. USA* **2016**, *113*, 8344–8353. [\[CrossRef\]](#)
31. Welkie, D.G.; Rubin, B.E.; Diamond, S.; Hood, R.D.; Savage, D.F.; Golden, S.S. A hard day's night: Cyanobacteria in diel cycles. *Trends Microbiol.* **2019**, *27*, 231–242. [\[CrossRef\]](#)
32. Omata, T.; Murata, N. Cytochromes and prenylquinones in preparations of cytoplasmic and thylakoid membranes from the cyanobacterium (blue-green alga) *Anacystis nidulans*. *Biochim. Biophys. Acta Bioenerg.* **1984**, *766*, 395–402. [\[CrossRef\]](#)
33. Mullineaux, C.W. Co-existence of photosynthetic and respiratory activities in cyanobacterial thylakoid membranes. *Biochim. Biophys. Acta Bioenerg.* **2014**, *1837*, 503–511. [\[CrossRef\]](#) [\[PubMed\]](#)
34. Berry, S.; Schneider, D.; Vermaas, W.F.J.; Rögner, M. Electron transport routes in whole cells of *Synechocystis* sp. Strain PCC 6803: The role of the cytochrome *bd*-type oxidase. *Biochemistry* **2002**, *41*, 3422–3429. [\[CrossRef\]](#) [\[PubMed\]](#)
35. Howitt, C.A.; Vermaas, W.F.J. Quinol and cytochrome oxidases in the cyanobacterium *Synechocystis* sp. PCC 6803. *Biochemistry* **1998**, *37*, 17944–17951. [\[CrossRef\]](#)
36. Shimakawa, G.; Shaku, K.; Nishi, A.; Hayashi, R.; Yamamoto, H.; Sakamoto, K.; Makino, A.; Miyake, C. FLAVODIIRON2 and FLAVODIIRON4 proteins mediate an oxygen-dependent alternative electron flow in *Synechocystis* sp. PCC 6803 under CO₂-limited conditions. *Plant Physiol.* **2015**, *167*, 472–480. [\[CrossRef\]](#)
37. Shimakawa, G.; Shaku, K.; Miyake, C. Oxidation of P700 in photosystem I is essential for the growth of cyanobacteria. *Plant Physiol.* **2016**, *172*, 1443–1450. [\[CrossRef\]](#)
38. Helman, Y.; Tchernov, D.; Reinhold, L.; Shibata, M.; Ogawa, T.; Schwarz, R.; Ohad, I.; Kaplan, A. Genes encoding A-type flavoproteins are essential for photoreduction of O₂ in cyanobacteria. *Curr. Biol.* **2003**, *13*, 230–235. [\[CrossRef\]](#)
39. Sétif, P.; Shimakawa, G.; Krieger-Liszkay, A.; Miyake, C. Identification of the electron donor to flavodiiron proteins in *Synechocystis* sp. PCC 6803 by in vivo spectroscopy. *Biochim. Biophys. Acta Bioenerg.* **2020**, *1861*, 148256. [\[CrossRef\]](#)
40. Hanawa, H.; Ishizaki, K.; Nohira, K.; Takagi, D.; Shimakawa, G.; Sejima, T.; Shaku, K.; Makino, A.; Miyake, C. Land plants drive photorespiration as higher electron-sink: Comparative study of post-illumination transient O₂-uptake rates from liverworts to angiosperms through ferns and gymnosperms. *Physiol. Plant.* **2017**, *161*, 138–149. [\[CrossRef\]](#)
41. Sejima, T.; Hanawa, H.; Shimakawa, G.; Takagi, D.; Suzuki, Y.; Fukayama, H.; Makino, A.; Miyake, C. Post-illumination transient O₂-uptake is driven by photorespiration in tobacco leaves. *Physiol. Plant.* **2016**, *156*, 227–238. [\[CrossRef\]](#)
42. Shimakawa, G.; Miyake, C. Oxidation of P700 ensures robust photosynthesis. *Front. Plant Sci.* **2018**, *9*, 1617. [\[CrossRef\]](#) [\[PubMed\]](#)
43. Shimakawa, G.; Miyake, C. Respiratory terminal oxidases alleviate photo-oxidative damage in photosystem I during repetitive short-pulse illumination in *Synechocystis* sp. PCC 6803. *Photosynth. Res.* **2018**, *137*, 241–250. [\[CrossRef\]](#) [\[PubMed\]](#)
44. Cooley, J.W.; Vermaas, W.F.J. Succinate dehydrogenase and other respiratory pathways in thylakoid membranes of *Synechocystis* sp. strain PCC 6803: Capacity comparisons and physiological function. *J. Bacteriol.* **2001**, *183*, 4251–4258. [\[CrossRef\]](#) [\[PubMed\]](#)
45. Schuurmans, R.M.; van Alphen, P.; Schuurmans, J.M.; Matthijs, H.C.P.; Hellingwerf, K.J. Comparison of the photosynthetic yield of cyanobacteria and green algae: Different methods give different answers. *PLoS ONE* **2015**, *10*, e0139061. [\[CrossRef\]](#)
46. Viola, S.; Bailleul, B.; Yu, J.; Nixon, P.; Sellés, J.; Joliot, P.; Wollman, F.-A. Probing the electric field across thylakoid membranes in cyanobacteria. *Proc. Natl. Acad. Sci. USA* **2019**, *116*, 21900–21906. [\[CrossRef\]](#)
47. Scherer, S.; Böger, P. Respiration of blue-green algae in the light. *Arch. Microbiol.* **1982**, *132*, 329–332. [\[CrossRef\]](#)
48. Ito, S.; Osanai, T. Unconventional biochemical regulation of the oxidative pentose phosphate pathway in the model cyanobacterium *Synechocystis* sp. PCC 6803. *Biochem. J.* **2020**, *477*, 1309–1321. [\[CrossRef\]](#)
49. Benson, P.J.; Purcell-Meyerink, D.; Hocart, C.H.; Truong, T.T.; James, G.O.; Rourke, L.; Djordjevic, M.A.; Blackburn, S.I.; Price, G.D. Factors altering pyruvate excretion in a glycogen storage mutant of the cyanobacterium, *Synechococcus* PCC7942. *Front. Microbiol.* **2016**, *7*, 475. [\[CrossRef\]](#)
50. Braakman, R.; Follows, M.J.; Chisholm, S.W. Metabolic evolution and the self-organization of ecosystems. *Proc. Natl. Acad. Sci. USA* **2017**, *114*, E3091–E3100. [\[CrossRef\]](#)
51. Eisenhut, M.; Ruth, W.; Haimovich, M.; Bauwe, H.; Kaplan, A.; Hagemann, M. The photorespiratory glycolate metabolism is essential for cyanobacteria and might have been conveyed endosymbiotically to plants. *Proc. Natl. Acad. Sci. USA* **2008**, *105*, 17199–17204. [\[CrossRef\]](#)
52. Shimakawa, G.; Kohara, A.; Miyake, C. Medium-chain dehydrogenase/reductase and aldo-keto reductase scavenge reactive carbonyls in *Synechocystis* sp. PCC 6803. *FEBS Lett.* **2018**, *592*, 1010–1019. [\[CrossRef\]](#) [\[PubMed\]](#)
53. Grimme, L.H.; Boardman, N.K. Photochemical activities of a particle fraction P₁ obtained from the green alga *Chlorella fusca*. *Biochem. Biophys. Res. Commun.* **1972**, *49*, 1617–1623. [\[CrossRef\]](#)
54. Elhai, J.; Wolk, C.P. A versatile class of positive-selection vectors based on the nonviability of palindrome-containing plasmids that allows cloning into long polylinkers. *Gene* **1988**, *68*, 119–138. [\[CrossRef\]](#)

-
55. Hayashi, R.; Shimakawa, G.; Shaku, K.; Shimizu, S.; Akimoto, S.; Yamamoto, H.; Amako, K.; Sugimoto, T.; Tamoi, M.; Makino, A.; et al. O₂-dependent large electron flow functioned as an electron sink, replacing the steady-state electron flux in photosynthesis in the cyanobacterium *Synechocystis* sp. PCC 6803, but not in the cyanobacterium *Synechococcus* sp. PCC 7942. *Biosci. Biotechnol. Biochem.* **2014**, *78*, 384–393. [[CrossRef](#)]
 56. Sakurai, I.; Mizusawa, N.; Wada, H.; Sato, N. Digalactosyldiacylglycerol is required for stabilization of the oxygen-evolving complex in photosystem II. *Plant. Physiol.* **2007**, *145*, 1361–1370. [[CrossRef](#)]
 57. Schreiber, U.; Schliwa, U.; Bilger, W. Continuous recording of photochemical and non-photochemical chlorophyll fluorescence quenching with a new type of modulation fluorometer. *Photosynth. Res.* **1986**, *10*, 51–62. [[CrossRef](#)]
 58. Van Kooten, O.; Snel, J.F.H. The use of chlorophyll fluorescence nomenclature in plant stress physiology. *Photosynth. Res.* **1990**, *25*, 147–150. [[CrossRef](#)]